Parameterising the multiscale structure of organised convection using a cellular automaton

Judith Berner*, Glenn Shutts†, Tim Palmer*

**ECMWF, Shinfield Park, Reading*
RG2 9AX, United Kingdom
berner@ecmwf.int

†*MetOffice, FitzRoy Road, Exeter*
EX1 3PB, United Kingdom

1 Introduction

Despite the success in recent years in improving numerical weather prediction and climate models, a satisfactory representation of the multiscale structure of tropical variablity continuous to be problematic. Tropical variability is organised by diabatic heating through convection and characterised by a number of interlocked phenomena that act on different spatial and temporal scales and involve complex multiscale interactions. The most dominant mode of tropical variability is the Madden-Julian-Oscillation (MJO), a multiscale phenomenon consisting of individual westward propagating cloud clusters embedded in an eastward propagating envelope. In global atmospheric models the variability associated with MJO tends to be too weak and does not have the right propagation speeds (Slingo et al., 1996; Tompkins and Jung, 2003). A better representation of the MJO in NWP and climate models is desirable, since it may affect extratropical predictability on the medium-range (Ferranti, 1990) and might impact the representation of El Niño events on climatic scales (e.g. Barnett, 1984).

There have been a number of studies involving cloud-resolving models (CRMs) that have shown convective organisation and MJO-like features (Grabowski, 2001; Shutts and Palmer, 2003), although there remains some doubt if the underlying processes resulting in these MJO-like features are the same as in nature. Nevertheless, the fact that these higher-resolution simulations produce convective organisation in the form of westward and eastward propagating disturbances is an indication that processes at or below the truncation scale of GCMs may play an important role in the dynamics of the MJO.

On way to account for the variability of unresolved processes is to represent them in a stochastic manner. In recent years there have been a number of efforts to include such stochastic parameterisations into atmospheric models (Buizza et al., 1999; Shutts and Palmer, 2003; Lin and Neelin, 2000). Typically, the subgrid-scale fluctuations are modelled by state-dependent or state-independent noise processes, which can have temporal and spatial correlations. Stochastic-dynamic parameterisations (Palmer 2001) take this concept a step further and introduce an independent dynamical model for subgrid-scale variability. In this case the subgrid state evolves according to its own dynamics, but is at the same time coupled to the resolved state over a range of scales.

The use of a class of relatively simple dynamical systems called cellular automata (CA) for this purpose has been proposed by Palmer (2001) and successfully implemented in the context of the stochastic backscattering of kinetic energy by Shutts (2004). Cellular automata consist of a number of gridded cells, whose discrete states are determined by a set of rule based on the temporal history of each cell and its immediate neighbours. Therefore they are capable of producing spatially coherent patterns with temporal correlations.

The purpose of this study is to see if a cellular-automaton based parameterisation for organised convection (CAPOC) coupled over a range of scales to the global model can improve the representation of MJO activity. In

particular we are interested in modelling processes that cannot be captured by classical bulk-parameterisations, such as mesoscale organisation, which can have spatial scales of hundreds of kilometres. Shutts and Gray (1994) studied these processes in a CRM and found that up to 30% of the kinetic energy released in convective heating is captured in a balanced mesoscale circulation field. The potential vorticity associated with this balanced flow has the signature of a dipole in the vertical with lower-level cyclonic and upper-level anticyclonic perturbations. To mimic this aspect of organised convection, we introduce the stochastic forcing into the non-divergent part of the model dynamics and give it a dipole structure in the vertical.

To introduce state-dependence we follow the proposal of Palmer (2001) and trigger the CAPOC in regions with large convectively available potential energy (CAPE), which is the amount of buoyant energy available to accelerate a parcel vertically. Previous work has shown that the ability of global models to produce strong westerly wind bursts and MJO is sensitive to the threshold value at which convective readjustment takes place (e.g., Vitard et al., 2003; Tompkins and Jung, 2003). Therefore CAPE seems to be a natural choice for linking the random perturbations from the CAPOC to the large-scale flow.

The study is structured as follows: Section 2 discusses the multiscale structure of tropical convection and demonstrates the ability of cellular automata to produce interlocked multiscale structures. CAPOC implementation and experimental setup are described in Section 3. Section 4 consists of some preliminary results, which are discussed in Section 5.

2 A multiscale cellular automaton mimicking organised convection

Out of the multitude of eastward and westward propagating tropical waves described in observational studies (e.g., Wheeler and Kiladis, 1999), we focus on the multi-scale structure of the most dominant disturbances. As a first approximation, tropical organised convection can be described in terms of individual cloud-clusters, that travel westward with a speed of 10-30m/s and have horizontal scales of 100km and are embedded in an eastward-propagating envelope of large-scale superclusters that have a spatial scale of a few thousand kilometres and speeds of 5-10m/s (e.g., Nakazawa, 1988). This multiscale structure is for example evident in Hovmoeller diagrams (Fig.1) of the velocity potential and zonal wind anomalies in the ERA-40 reanalysis data (Uppala et al.2005).

Here we give an example that a coupled system of two interacting cellular automata each governed by a set of simple rules can produce multiscale behaviour reminiscent of that observed in nature. The multiscale cellular automation is composed of two cellular automata that evolve on different spatial scales and are governed by different rules (Palmer 2001): the small-scale CA mimics the westward propagation of individual cloud-clusters, while the intermediate scale CA describes their eastward propagating envelope. The rules governing the internal organisation of the small-scale cellular automaton are those developed by Shutts and Palmer (2003), whose work is referred to for details. The automaton is defined on a linear latitude-longitude grid and each cell can be either alive or dead. A cells that has the maximum number of possible lives is called a fertile cell. The maximal number of lives N, here N=32, is the only parameter of the model and influences the temporal memory of the cellular automaton. Depending on the number of fertile cells in an immediate neighbourhood and the state of the cell itself, the rules determine if a new fertile cell is born and under which circumstances a cell survives. Each cell of the automaton is then updated after each timestep. The internal rules for the small-scale automaton are chosen, so that the resulting patterns have features reminiscent of cloud clusters: they form distinct fronts spanning several grid cells and develop regions of high and low density. A westward propagation of these "cloud clusters" is enforced by an additional rule that consists of shifting all cells after each timestep Δt by 1° to the left, which corresponds to a propagation speed of v $\approx$ 15 m/s.

The intermediate-scale CA is very coarse and has a gridlength of 40°. The cells of the intermediate-scale CA can be either 'off' or 'on' and the only rule is that the cells are shifted after each timestep Δt by 2° corresponding to a eastward propagating envelope of cloud clusters. The two cellular automata are coupled to each other by one single rule, namely, that a new fertile cell in the small-scale CA can only be born, if the intermediate-scale

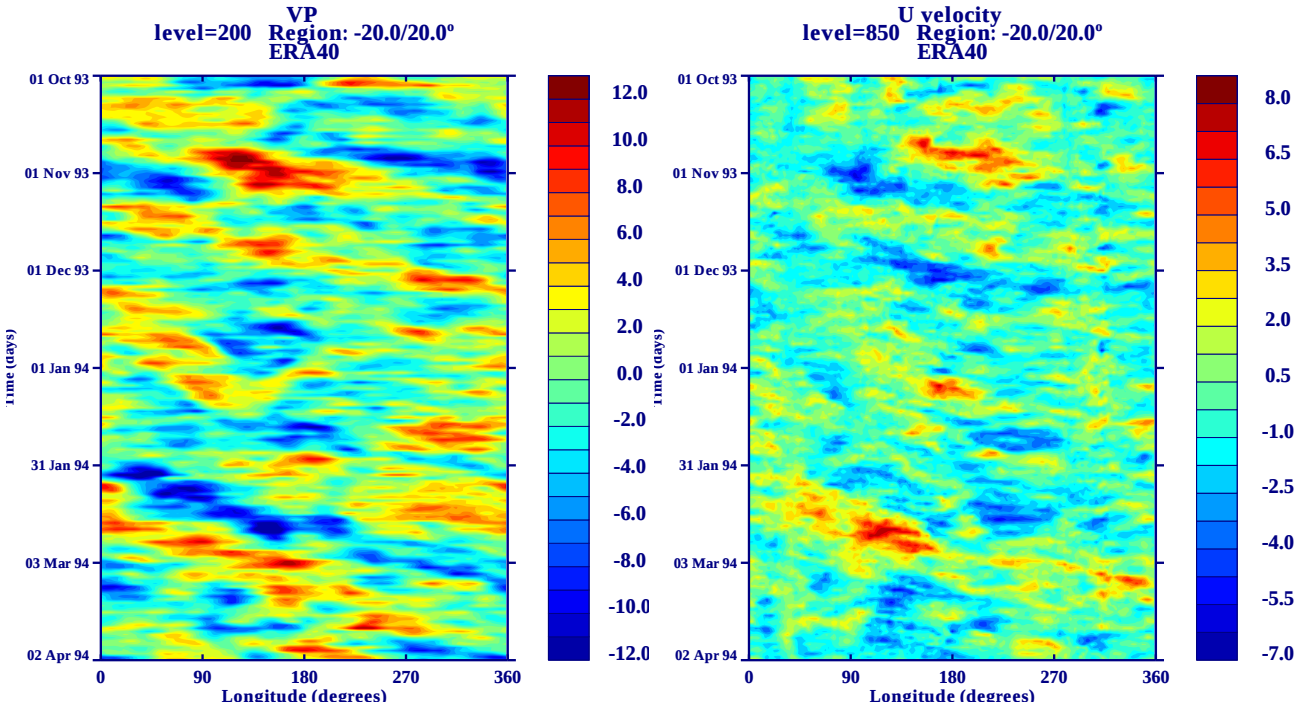

Figure 1: Hovmoeller diagrams of daily data of velocity potential anomalies in the 200hPa pressure level (left panel) and zonal wind anomalies (m/s)in 850hPa (right panel) from the ERA-40 reanalysis for the extended winter season 1993/1994. The anomalies are averaged over the tropical latitude band $20\,^{\circ}S$ *to* $20^{\circ}N$.

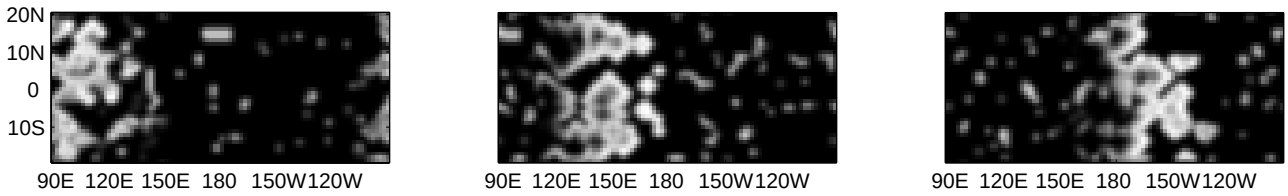

Figure 2: Snapshots of horizontal pattern organisation in a multiscale cellular automaton (MSCA) for organised convection at three different times.

CA is 'on'.

The evolution of this multiscale cellular automaton (MSCA) for convective organisation at three different times after an initial spin-up time is given in Fig.2. On the finest scale individual cloud clusters are detectable. These cloud clusters organise in eastward propagating super clusters. The multiscale structure of the MSCA with small convective cells propagating to the west at a speed of $v \approx 12.5$ m/s while their envelope propagates to the east at $v \approx 5$ m/s becomes evident in the Hovmoeller digram (Fig. 3).

3 Implementation and Experimental Setup

The cellular automaton based parametrisation for organised convection (CAPOC) has been implemented into the atmospheric model component of the European Centre for Medium-Range Weather Forecasts (ECMWF) Integrated Forecasting system (IFS) in the following manner. First, the small-scale cellular automaton of Sec-

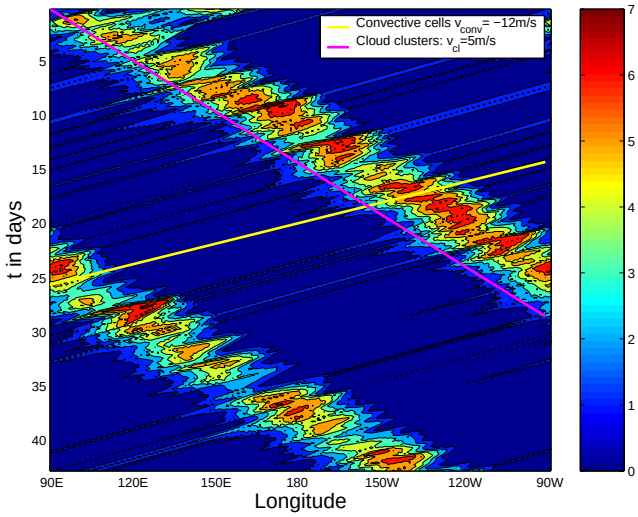

Figure 3: Hovmoeller diagram of the structures modelled by the multiscale cellular automaton in Fig.2

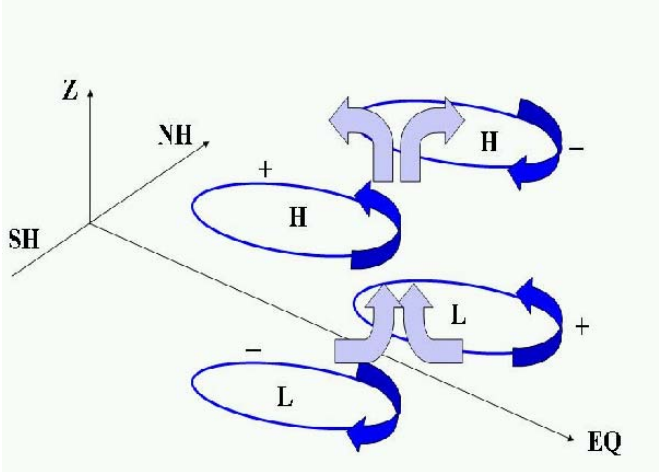

Figure 4: Schematic of vorticity generation and pressure perturbations associated with diabatic heating at the equator

tion 2 is used to generate random patterns Ψ that have spatial and temporal correlations. To introduce eastward propagation with a speed of v $\approx$ 5 m/s the cells are shifted after each timestep $\Delta t = 1$h by 0.5° to the right. To efficiently interact with the large-scale flow, but not explicitly introduce divergence, we closely follow Shutts (2004) and interpret the so generated pattern as divergence-free streamfunction forcing.

Convective organisation is driven by diabatic heating of the mid-troposphere over convectively active regions, which is associated with positive vertical motion leading. For continuity reasons, this results in tropospheric upper-level divergence and low-level convergence. Due to the divergence term in the vorticity equation and given that absolute vorticity is positive for disturbances in the Northern hemisphere and negative for disturbances in the Southern hemisphere, the diabatic heating will result in cyclonic vorticity generation on the lower troposphere and anticyclonic vorticity generation in the upper troposphere (e.g., Holton, 1992). These theoretical considerations are confirmed by the explicit integrations of CRMs (Shutts and Gray 1994). Although a simplification of more careful studies (e.g. Moncrieff, 2004), the vorticity generation associated with convection at the equator is schematically shown in Fig.4. Note, that cyclones are associated with positive vorticity ξ in the Northern hemisphere (NH), but negative vorticity in the Southern hemisphere (SH) and, since $\xi = \nabla^2 \psi$, negative vorticity generation corresponds to a positive streamfunction forcing and vice versa.

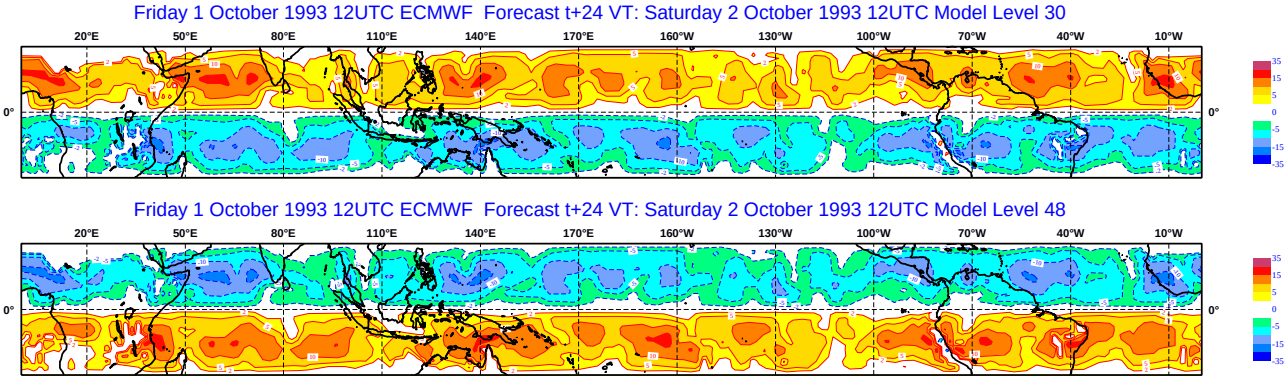

Figure 5: Horizontal structure of streamfunction forcing in the upper (top panel) and lower (bottom panel) troposphere before multiplication with CAPE.

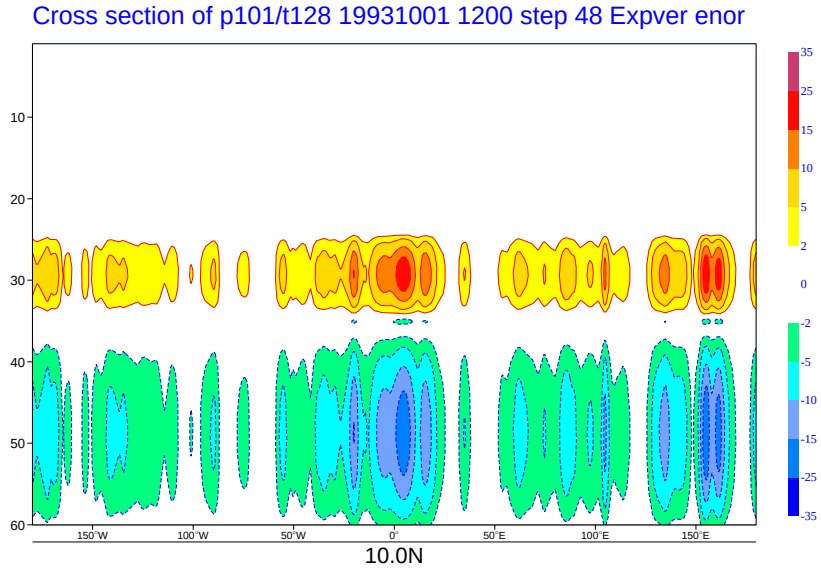

Figure 6: Vertical cross-section of the streamfunction forcing at 10N before multiplication with CAPE.

Consist with these considerations, the CA patterns Ψ are multiplied by sine functions to have a dipole structure in the horizontal as well as in the vertical. Together with the vertical modulation this results in a positive streamfunction forcing in the upper levels of the NH and the lower levels of the SH and a negative streamfunction forcing in the lower levels of the NH and the upper levels of the SH (Fig.5). In the horizonal the forcing is confined to the tropical band between 20°S and 20°N.

The vertical structure is that of a dipole with extrema at model levels 30, corresponding to the 215hPa-level or $\approx$ 11km, and 48 corresponding to 870hPa in $\approx$ 1.4km. One realization of the vertical cross-section of the streamfunction forcing at a latitude of 10N is shown in Fig.6.

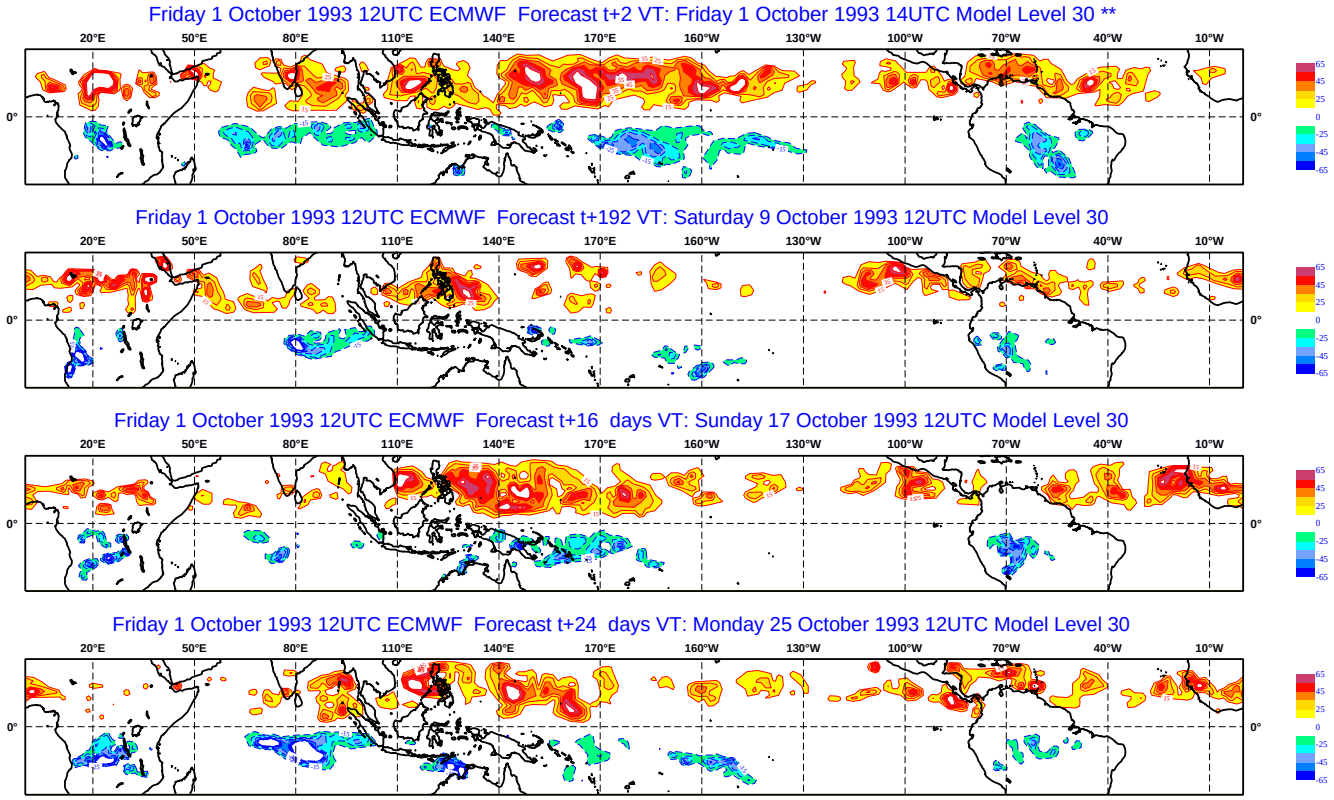

Figure 7: Sequence of streamfunction forcing after 2h, 10d, 20d and 30d at model level 30 (ca. 215hPa).

To trigger the CAPOC over regions with strong convective potential and make the parameterisation state-dependent, the streamfunction forcing is subsequently multiplied with the strength of convectively available potential energy (CAPE)

$$d\psi/dt = CAPE(\lambda,\phi) * f(\Psi(\lambda,\phi),z)\,. \tag{1}$$

where λ and ϕ are the geographical longitude and latitude, and f the horizontal and vertical structure function. This streamfunction forcing is then transformed into spectral space, expressed as a vorticity increment $\Delta\xi = \Delta(\nabla^2\psi)$ and added to the prognostic equations for relative vorticity, which is a model variable (see also Shutts, 2004). Snapshots of the resulting upper-tropospheric streamfunction forcing after 2h, 10d, 20d and 30d for a forecast starting Oct 1, 1993 are shown in Fig.7. Due to the weighting with CAPE, the forcing is strongest over the west Pacific and tends to be stronger in the Northern hemisphere than in the Southern.

The CA based parametrisation for convective parametrisation (CAPOC) has been implemented into the IFS, version CY28R3. It was integrated using 60 vertical levels and at a horizontal resolution of T_L95 (linear Gaussian grid with gridlength $\equiv 1,875^{\circ}$) and uses observed SSTs as lower boundary conditions. Two experiments were conducted, one control experiment and one with the CAPOC scheme. Each experiments was started on Oct 1 of each of the years 1962-2001 and integrated for a total of 6 months, which amount to a total of 40 extended winter seasons. Due to its importance for understanding tropical dynamics, we focus on the velocity potential in 200hPa (VP200) in the region between 20°S and 20°N.

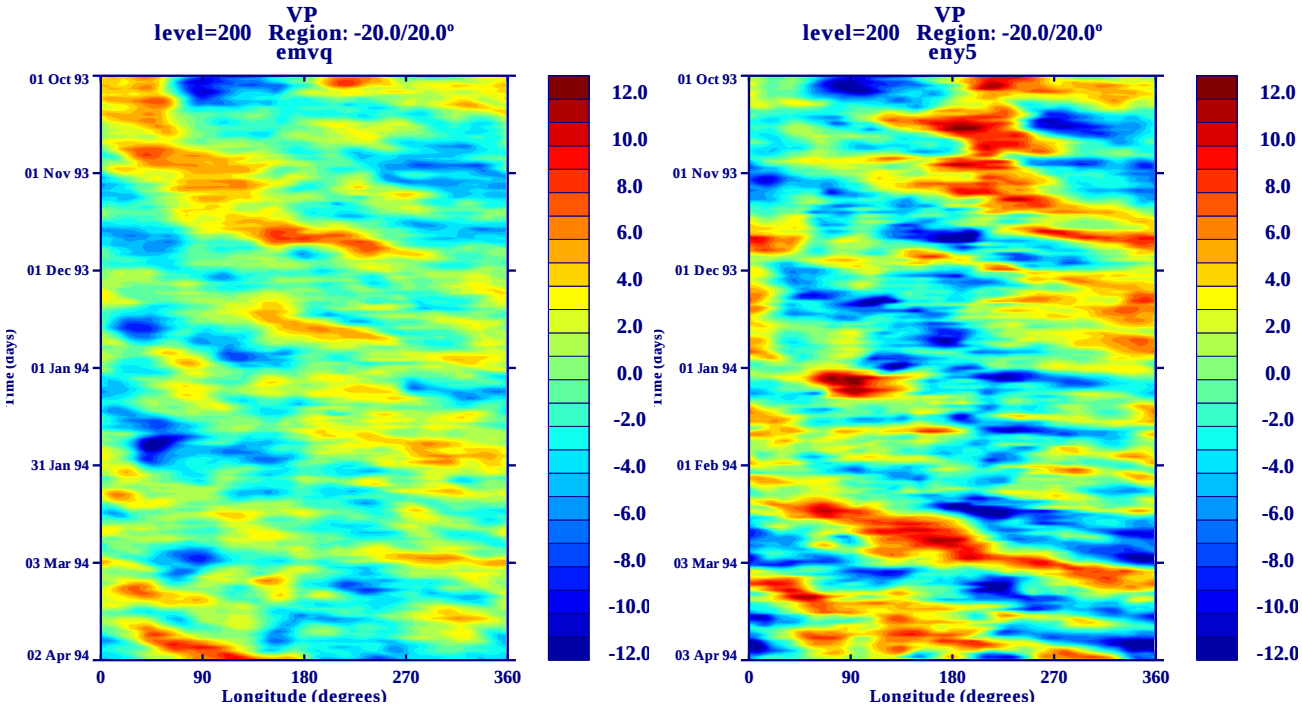

Figure 8: Hovmoeller diagram of tropical velocity potential anomalies in 200hPa for IFS Control (left panel) and IFS with cellular automaton based convective parameterisation (CAPOC) (right panel). All other conventions as in Fig.1.

4 Preliminary results

To see the qualitative difference in observed and modelled tropical variability, Hovmoeller diagrams of VP200-anomalies for the winterseason 1993/94 are calculated. Although the model is started from observed initial conditions, the tropical atmosphere is not predictable beyond the first two weeks or so. Therefore we do not focus on any individual features in the Hovmoeller diagrams, but their general characteristics. The regions of strong upper-level divergence in the ERA40 data indicated by negative velocity potential in the upper troposphere confirm that this winter season had several strong MJO events (Fig. 1). The model shows some MJO activity at the beginning of the integration, but exhibits the known shortcomings: the anomalies do not propagate into the Eastern Pacific and have too little amplitude (Fig.8, left panel). This is changed in the CAPOC-experiments (Fig.8, right panel): now the velocity-potential anomalies have similar amplitudes as the observations and there appears a strong MJO-type disturbance developing after five months, which is propagating across the date line into the West Pacific at approximately the right speed. The scheme has introduced variability at smaller spatial and temporal scales, but apparently too much east of the dateline.

The streamfunction forcing during this 6-month period is shown for the meridionally-averaged region between the equator and 20°N in Fig.9 (left panel). The CAPE-weighting has lead to an intermittent forcing, which is mostly confined to the convective area over the Western Pacific. The influence of the cellular automaton is visible as weak disturbances in form of westward and eastward propagating streaks. These eastward and westward propagating features are more clearly visible in the Hovmoeller diagram of the corresponding CA-pattern for the first three months of this season (Fig.9, right panel). The eastward propagating features are tuned to have a period of about 30d, while the westward propagating features are smaller scale and have more than one characteristic timescale.

To see if these impressions are confirmed if 40 years of data are analysed, spectra as function of longitude are computed. The ERA40 reanalysis data show a clear spectral peak between 60°E and180°E for periods between

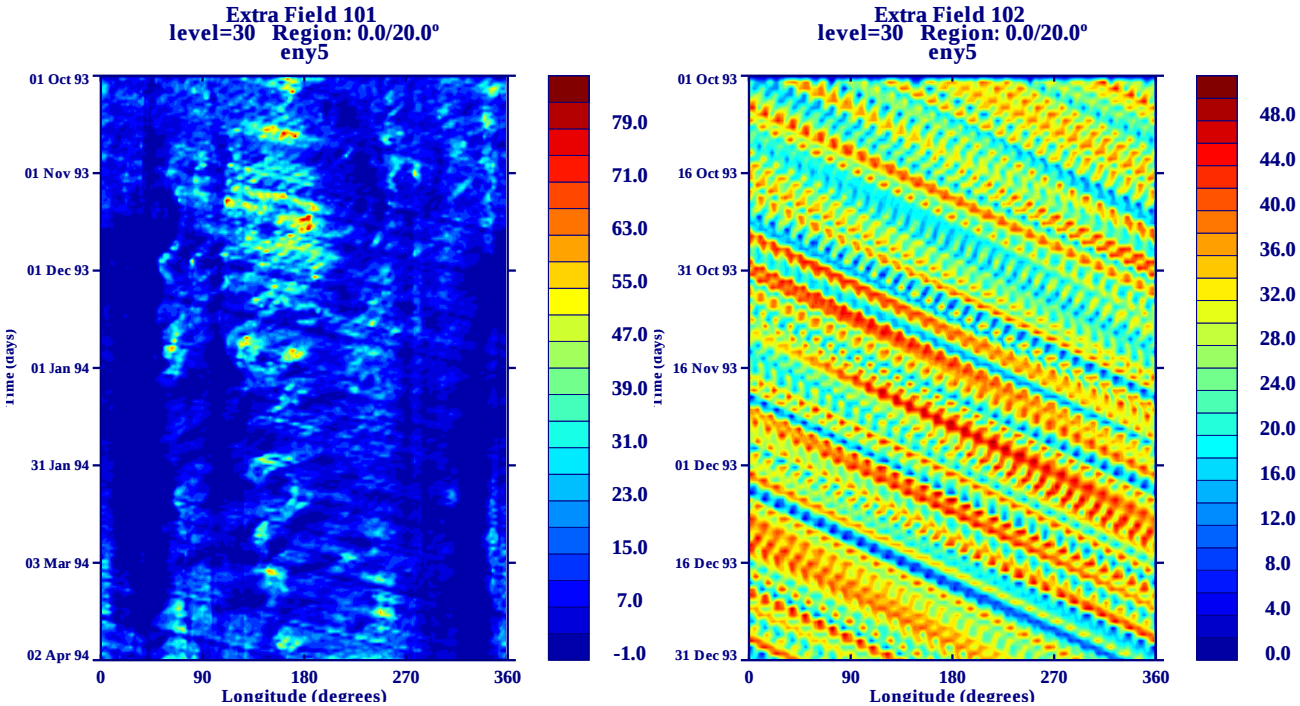

Figure 9: Left panel: Hovmoeller diagram of the streamfunction forcing from CAPOC for the extended winter season 1993/1994. The anomalies are averaged over the tropical latitude band 0 to 20 °N. Right panel: Hovmoeller diagram of CA-pattern before weighting with CAPE for a three month period.

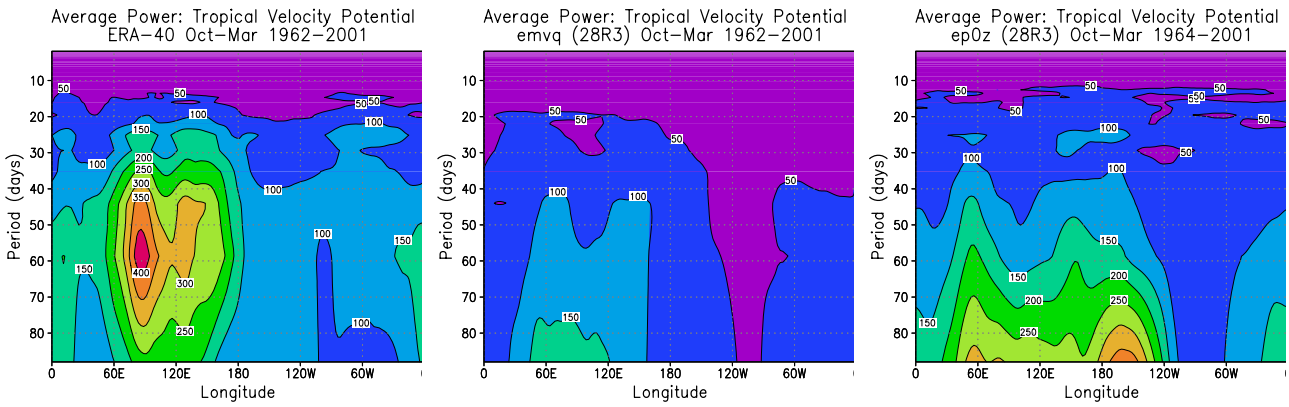

Figure 10: Power spectra of velocity potential as function of longitude

40 and 70 days (Fig.10, left panel). As previously reported by Jung et al. 2005, the model does not produce this spectral peak (Fig.10, middle panel), but has a red power spectrum at all longitudes. The spectral power is generally too small, but the model captures the fact that there is more variability in the Western Pacific than east of the dateline. As already seen in the Hovmoeller diagrams, the variability is greatly enhanced if the model is run with the CAPOC-scheme (Fig.10, right panel). There is still no peak for periods between 40 and 70 days, but the amplitude of the spectrum in this period range has increased considerably, e.g., by a factor of two for a period of 60d. However, the scheme has introduced strong and erroneous variability between 180°W and 120°W.

5 Summary and Discussion

Following the proposal of Palmer 2001, a first attempt was made to develop a stochastic-dynamic parametrisation for convective organisation using a cellular automaton. The CA-based convective parametrisation tries to model the essence of organised convection by combining physical insights with random elements to mimic certain aspects of tropical variability. Certainly, a less empirical approach would be desirable, but the explicit integration of 3D cloud resolving models on the global domain is not computationally feasible in the near future. Alternatively, mathematically stringent methods to accurately describe subgrid-scale fluctuations developed in the stochastic community and recently applied to simplified models of atmospheric dynamics (e.g, Majda et al. 2003; Berner, 2005; Franzke and Majda 2005) are difficult to apply because of the high-dimensionality and complexity of GCMs.

As a stochastic-dynamic model for sub- and supergrid variability, a cellular automaton was used to generate a quasi-random perturbation field with coherent spatial patterns and temporal memory. To efficiently interact with the large-scale flow we closely follow Shutts (2004) and interpret the patterns as streamfunction forcing. Aimed at modelling processes not captured by current convective parameterisations, like the outflow of convective organisation, the streamfunction perturbations are given a horizontal and vertical structure mimicking the signature of convective heating (Shutts and Gray, 1994; Gill, 1980; Moncrieff, 2004). Since these processes can have spatial scales of hundreds of kilometres, CAPOC lies much beyond the classical notion of stochastic parameterisations as representing subgrid-scale fluctuating and is coupled to the resolved flow over a range of scales including the subgrid-, near- and super-grid scales. The implementation of CAPOC as streamfunction forcing in spectral space provides the possibility to study the multiscale coupling in more detail in the future.

To make the parametrisation state-dependent, the forcing is weighted by amount of CAPE, so that the CAPOC is triggered in regions, that are potentially convectively active. Previous studies have pointed out that the lack of intraseasonal variability may be due to the fact that the atmosphere is too stable and that the strength of westerly windbursts and convective organisation can be considerably increased if a higher CAPE-threshold for convective adjustment is used (e.g., Vitart et al. 2003). Having a larger threshold delays the onset of deep convection, but at the same time allows for deeper and stronger convection, once it is triggered. Due to its design, CAPOC adds perturbations over convectively active regions and thus makes the atmosphere less stable, but lacks the element of a build up of potential energy for deeper convection.

A first implementation suggests that CAPOC impacts tropical variability and changes the amplitude of propagating eastward disturbances evident in velocity potential and u850 wind anomalies. As it stands CAPOC has increased the power spectral density for periods between 40 and 70 days, but has failed to introduce a spectral peak for these periods. Obviously the results shown are of a very preliminary nature and a more in-depth analysis is needed to see if the spectral characteristics and multiscale structure of the convectively coupled disturbances are indeed improved. Should this be the case, CAPOC provides a simple framework to study the role of different key elements of the parameterisation, such as the vertical and horizontal structure of the streamfunction forcing, its spatial and temporal scales and the importance of nonlocality in the form of an imposed propagation speed.

Acknowledgements

Adrian Tompkins, Thomas Jung, Laura Ferranti, Frédéric Vitart and Martin Leutbecher are thanked for delightful discussions and help with running the ECMWF model. Mitch Moncrieff provided invaluable insight about organised convection and is thanked for comments on an earlier draft. Thanks to Adrian Tompkins and Thomas Jung who provided the diagnostics tools.

References

Barnett, T. P., 1986: *Origins of the Southern Oscillation*, Annual Climate Diagnostics Workshop, Ontario, Canada, NOAA, pp. 155–158.

Berner, J., 2005: Linking nonlinearity and non-gaussianity of planetary wave behavior by the Fokker-Planck equation, *J. Atmos. Sci.*, **62**, 2098–2117.

Buizza, R., M. Miller, and T. Palmer, 1999: Stochastic representation of model uncertainties in the ecmwf ensemble prediction system, *Quart. J. Roy. Meteor. Soc.*, **125**, 2887–2908.

Ferranti, L., T. N. Plamer, and F. M. E. Klinker, 1990: Tropical-extratropical interaction associated with the 30-60 day oscillation and its impact on medium and extended range prediction, *J. Atmos. Sci.*, **47**(18), 2177–2199.

Franzke, C., A. J. Majda, and E. Vanden-Eijnden, 2005: Low-order stochastic mode reduction for a realistic barotropic model climate, *J. Atmos. Sci.*, **62**, 1722–1745.

Gill, A. E., 1980: Some simple solutions for heat-induced tropical circulations, *Quart. J. Roy. Meteor. Soc.*, **106**, 447–462.

Holton, J. R., 1992: *Introduction to Dynamic Meteorology*, Academic Press, San Diego.

Jung, T., A. M. Tompkins, and M. J. Rodwell, 2005: Some aspects of systematic error in the ECMWF model, *Atmos. Sci. Lett.*, **6**, 133–139.

Lin, J. W. B. and J. D. Neelin, 2000: Influence of a stochastic moist convective parameterization on tropical climate variability, *Geophys. Res. Lett.*, **27**, 3691–3694.

Madden, R. A. and P. R. Julian, 1972: Description of global-scale circulation cells in the tropics with a 40-50 day period, *J. Atmos. Sci.*, **6**, 1109–1123.

Majda, A., I. Timofeyev, and E. Vanden-Eijnden, 2003: Systematic strategies for stochastic mode reduction in climate, *J. Atmos. Sci.*, **60**, 1705–1722.

Moncrieff, M. W., 2004: Analytic representation of the large-scale organization of tropical convection, *J. Atmos. Sci.*, **61**, 1521–1538.

Palmer, T. N., 2001: A nonlinear dynamical perspective on model error: A proposal for non-local stochastic-dynamic parameterization in weather and climate prediction, *Quart. J. Roy. Meteor. Soc.*, **127**, 279–304.

Shutts, G. J., 2004: A stochastic kinetic energy backscatter algorithm for use in ensemble prediction systems, *ECMWF Technical Memorandum*, **449**, available at http://www.ecmwf.int/publications/.

Shutts, G. J. and M. E. B. Gray, 1994: A numerical modelling study of the geostrophic adjustment following deep convection, *Quart. J. Roy. Meteor. Soc.*, **120**, 1145–1178.

Shutts, G. J. and T. N. Palmer, 2003: The use of high resolution numerical simulations of tropical circulation to calibrate stochatsic physics schemes, in *ECMWF/CLIVAR workshop on simulation and prediction of intra-seasonal variability with the emphasis on the MJO*, ECMWF, available from http://www.ecmwf.int/publications, pp. 83–102.

Slingo, J. M., K. R. Sperber, J. S. Boyle, J. P. Ceron, M. Dix, B. Dugas, W. Ebisuzaki, J. Fyfe, D. Gregory, J. F. Gueremy, J. Hack, A. Harzallah, P. Inness, A. Kitoh, W. K. M. Lau, B. McAvaney, R. Madden, A. Matthews, T. N. Palmer, C. K. Park, D. Randall, and N. Renno, 1996: Intraseasonal oscillations in 15 atmospheric general circulation models: Results from an AMIP diagnostic subproject, *Clim. Dyn.*, **12**, 325–357.

Tompkins, A. M. and T. Jung, 2003: Influence of process interactions on MJO-like convective structures in the IFS model, in *ECMWF/CLIVAR workshop on simulation and prediction of intra-seasonal variability with the emphasis on the MJO*, ECMWF, available from http://www.ecmwf.int/publications, pp. 103–114.

Vitart, F., M. A. Balmaseda, L. Ferranti, and D. Anderson, 2003: Westerly wind events and the 1997/98 El Nino event in the ECMWF seasonal forecasting system: A case study, *J. Climate*, **16**, 3153–3170.